paths starting with widely different initial conditions. This strongly suggests that this state of motion is stable. Probably it is unique for ordinary launchings. It is plausible that each boomerang has a characteristic final state of motion. For instance, flight path calculations made for boomerang 195.1 (level 3) yielded a final state characterized by the values:

$$f = 9.2 \text{ rev/s}, \; V = 13.5 \text{ m/s}, \; U = 0.78, \; \Psi = 9.2^\circ, \; -\vartheta = 61^\circ, \; \psi = 161^\circ,$$

$$\varphi = 18.4 \; , \; \Delta Z = 22.1 \text{ m}, \; \Delta t = 4.7 \text{ sec}.$$

Necessary conditions for a boomerang's final state of motion are:

$$\dot{V} = 0, \; \dot{\omega}_z = 0, \; \dot{\Psi} = 0, \; \dot{\vartheta} = 0, \; \dot{\psi} = 0. \qquad (28.1)$$

These are 5 equations for the 5 unknowns V, ω_z, Ψ, ϑ, ψ. The equations can be solved by putting the right-handed sides of the equations (4.8) and (4.9) equal to zero. If (28.1) is satisfied, $\dot{\varphi}$ = constant according to (4.9), and $\dot{Z}$ = constant while $\dot{X}$ and $\dot{Y}$ vary harmonically with φ according to (4.10). We shall not discuss the conditions for the existence, the stability, or the uniqueness of a boomerang's final state of motion.

In the boomerang flight presented in this section, the path curves counterclockwise (φ increases) until $t = 6.2$ sec. ($Z = 4.6$ m); after this φ decreases and the path curves clockwise. In other cases this reversal may occur at an earlier or at a later instant. This phenomenon can often be observed in real boomerang flights. Sometimes a boomerang may be well on its way to its final state of motion before it hits the ground. Curiously, the first counterclockwise loop, so characteristic for the flight of a right-handed boomerang, may be considered as merely a transient form of motion, soon leading up to the boomerang's final state.

In the final state of motion discussed above, the gravitational force plays a crucial role. What would happen in the absence of gravity? In the following we shall suppose that $g = 0$, that the air is homogeneous (with density $\mu = 1.20$ kg/m^3), and that there is no wind. The equations of motion (4.8), (4.9), (4.10) now are modified in an important aspect: for a given boomerang $\dot{V}$, $\dot{\omega}_z$ and $\dot{\Psi}$ depend only on the aerodynamic forces, and hence (in our model) only on V, ω_z and Ψ. The shape of the boomerang's flight path is independent of ϑ_o, φ_o, ψ_o, X_o, Y_o, Z_o. The path in

(Ψ,U)-space traversed by the boomerang depends only on Ψ_o and U_o, while V_o (or f_o) determines the velocity at which this path is traversed.

A necessary condition for Ψ being stationary is given by (22.1), and for U being stationary by (22.2). The restriction $\vartheta = \frac{1}{2}\pi$, $\psi = 0$ is not relevant now because gravity is absent. The boomerang will travel to a point with $\dot{\Psi} = 0$, $\dot{U} = 0$: (Ψ^*,U^*) (under conditions not investigated by us). Because the boomerang continually loses kinetic energy V and ω_z (or f) decrease. Since $\dot{V}(:) - V^2$, V decreases inversely with time, and the boomerang's path length increases logarithmically with time. The boomerang ends up moving, slower and slower, along a helical path, away to infinity.

A gravitationless flight for boomerang 101.1 was computed with the initial conditions: $f_o = 10$ rev/s, $V_o = 25$ m/s, $\Psi_o = 0°$. This boomerang's final motion is characterized by:

$$\Psi^* = 2.0°, \quad U^* = 0.86$$

and the helical path by:

$$\emptyset = 34 \text{ m}, \quad \Delta R = 31 \text{ m}, \quad \Delta P = 112 \text{ m}, \quad \Delta n = 70$$

where $\emptyset$ is the diameter of the helix, ΔR is the difference in the boomerang's position, ΔP the path length and Δn the number of revolutions between two points one turn of the helix apart. The helix is traversed clockwise as seen from the point of launching. The direction of the helix' axis depends on ϑ_o, φ_o and ψ_o. The helical motion begins rather soon after the start: already at $t = 7$ sec. we have $\Psi = 2.0°$, $U = 0.86$. At $t = 18.3$ sec. the boomerang has completed 100 spin revolutions and $f = 2.9$ rev/s, $V = 4.7$ m/s. At $t = 94.1$ sec. 200 revolutions are completed and $f = 0.7$ rev/s, $V = 1.1$ m/s.

The relative simple shape of the flight path in the gravitationless case is due to the fact that the motion proceeds at constant values for Ψ and U. In the presence of gravity there is no fixed equilibrium point (Ψ^*,U^*), and the boomerang moves about in the (Ψ,U)-plane. Much of the charm of real boomerang flights originates from the interplay of aerodynamic and gravitational forces.

§29 *Wind.*

In the practice of boomerang throwing the influence of wind on the boomerang's flight can be an important factor. Even a very light breeze of 1 m/s may significantly alter the shape of a flight path. In the absence of wind it does not matter whether the boomerang is thrown to the south or to the north; the flight path will have the same shape. As soon as there is wind, the direction in which the boomerang is launched does matter, and the angle φ_o may be a very important parameter indeed. If the wind is too strong, a boomerang's performance may be spoilt, the boomerang is taken with the wind and invariably lands at a considerable distance downwind. On the other hand, a moderate breeze may assist a boomerang in coming back. After carrying out a few trial throws in which the angle φ_o is varied, the boomerang thrower may obtain perfect return flights. This is particularly pleasing if the boomerang in case is incapable of returning well under windless conditions. Usually the optimum launching conditions are such that $\beta - \varphi_o \approx 45°$ (β determines the wind's direction, see §8).

Two such cases are shown in fig. 29.1 and fig. 29.2. The 4 flight paths are computed for boomerang 245.1 (level 3), which is associated with boomerang L5, see §18. For the flights of fig. 29.1 the initial conditions are:

$f_o = 10$ rev/s, $V_o = 25$ m/s, $\Psi_o = 0$,

$\vartheta_o = 80°$, $\varphi_o = 0°$, $\psi_o = -20°$,

$X_o = 0$ m, $Y_o = 0$ m, $Z_o = 1.8$ m,

a) no wind,

b) $\beta = 45°$, $W_o = 1.3$ m/s, $W_1 = 0{,}6$ m/s/10 m.

In the flights of fig. 29.2 the initial conditions are the same, except that $\vartheta_o = 70°$, $\psi_o = -30°$.

	wind	t	P	n	D	Z_2	D_2	D_1	f_2	f_1	V_1'	Ψ_2'	U_1'
29.1	no	10.1	112.6	98.5	17.6	13.4	44.1	15.7	10.6	9.0	2.0	80.9	.10
	yes	9.9	121.9	94.6	1.2	15.9	41.1	0.9	10.3	8.9	2.9	80.1	.09
29.2	no	12.2	114.2	122.1	24.1	16.1	39.2	20.5	11.1	9.0	2.4	64.8	.11
	yes	13.3	122.0	134.0	4.3	18.0	34.0	2.6	11.3	9.0	2.1	52.8	.13

table 29.1. Some values for the flights of fig. 29.1 and 29.2.

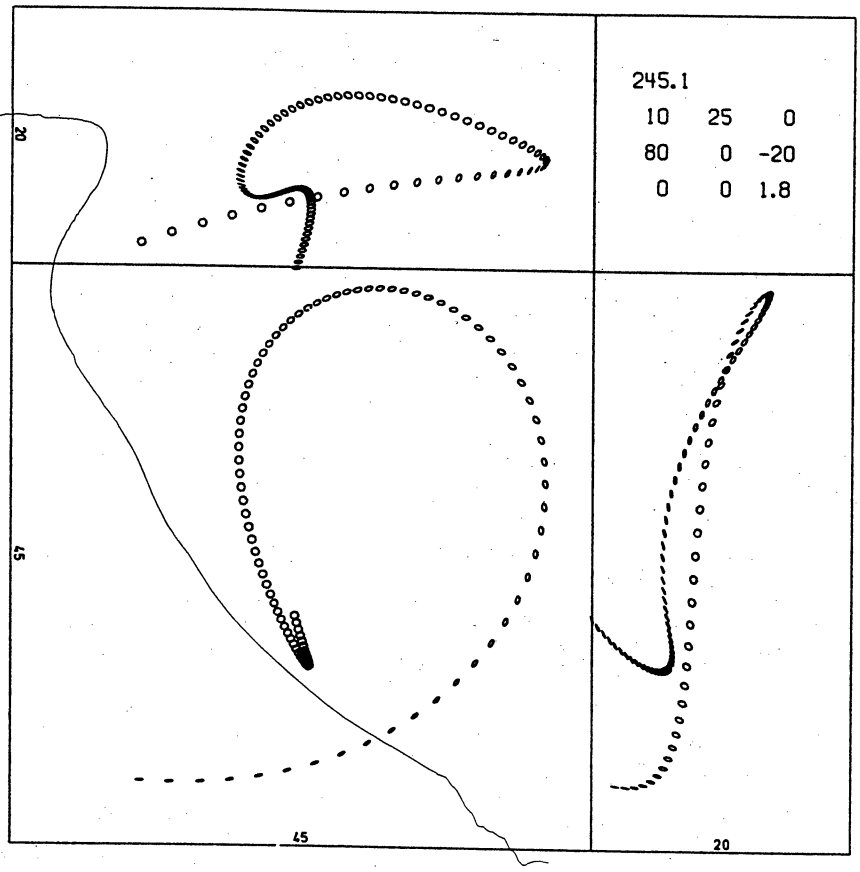

fig. 29.1a

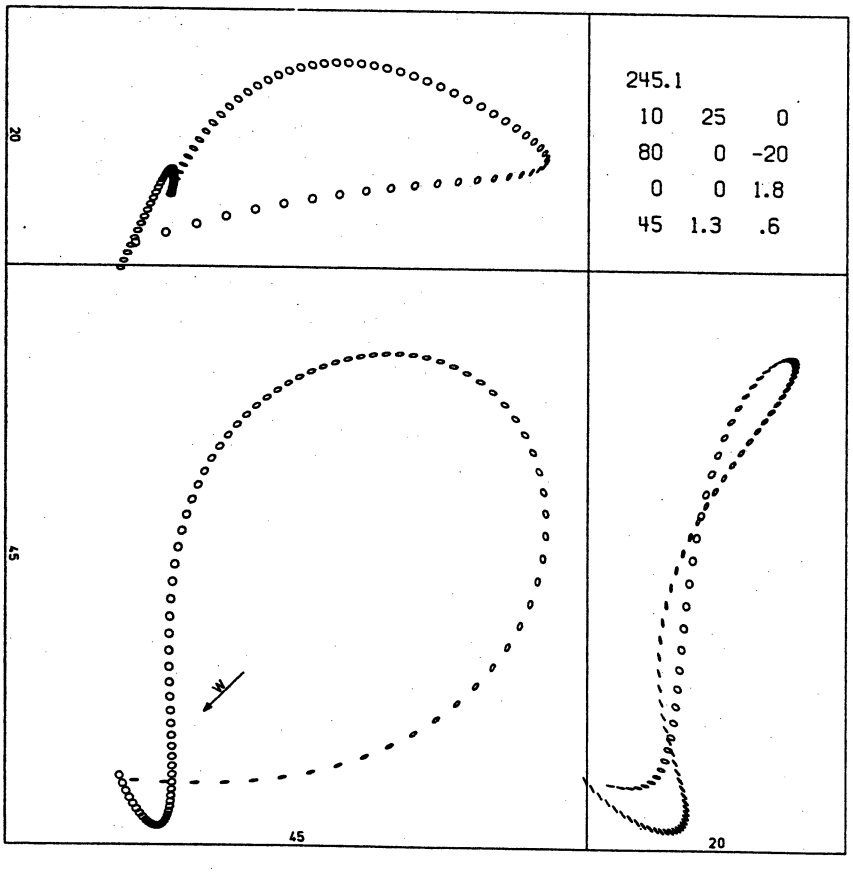

fig. 29.1b

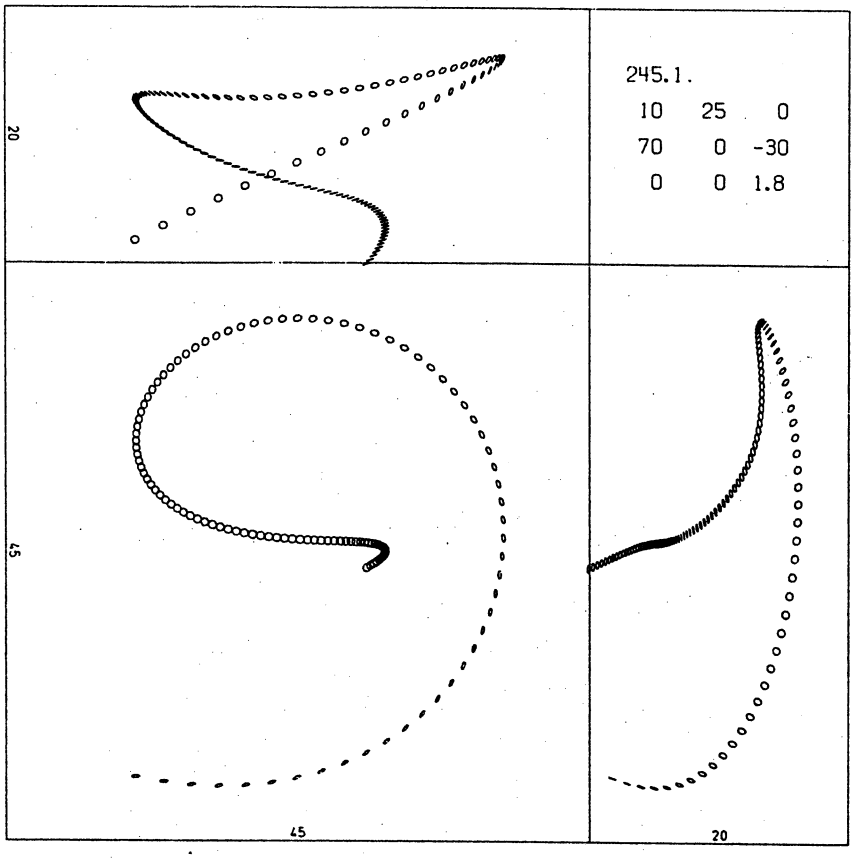

fig. 29.2a

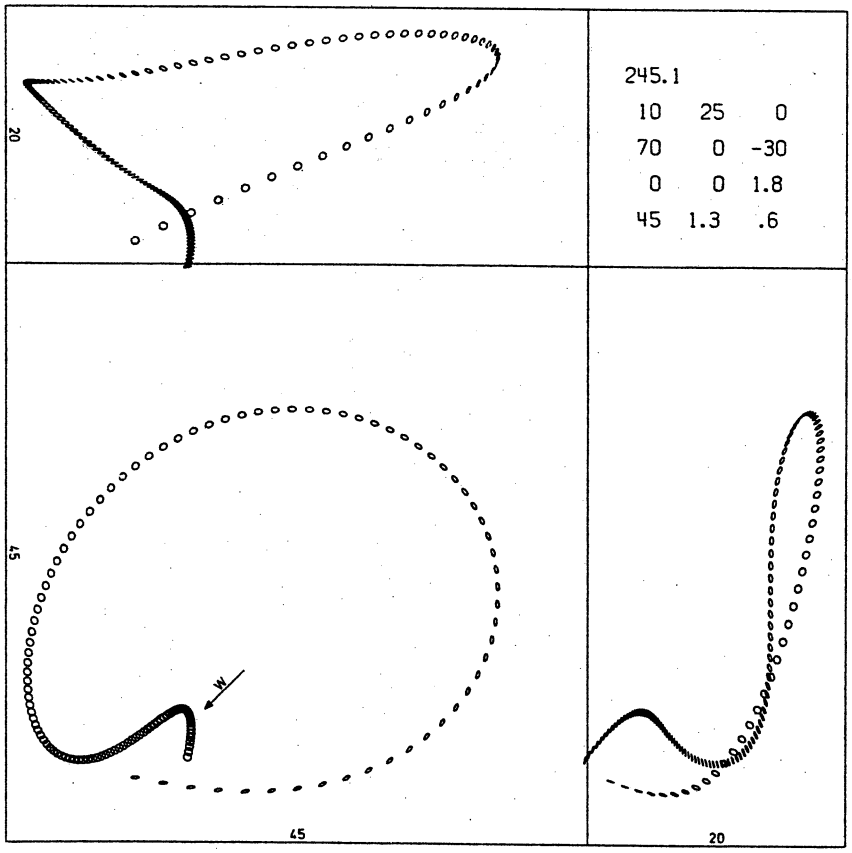

fig. 29.2b

Some values for these 4 flights are listed in table 29.1. In these examples the light breeze helps the boomerang to return beautifully.It is rather unfortunate that the field experiments with boomerang L5 (see §18) did not produce level 1 flight paths suitable for determining the influence of wind.

The main influence of the wind on a boomerang's flight can be explained as follows. Suppose the wind velocity field is constant and homogeneous ($W_1 = 0$). Use a coordinate system (X',Y',Z') moving with the air. In this inertial frame the air is motionless. However, the initial conditions for the boomerang's flight are modified: V_o, Ψ_o and U_o have to be replaced by V_o', Ψ_o' and U_o' according to §8. For instance, if a boomerang is launched directly into the wind, $V_o' > V_o$ and $U_o' > U_o$. In the (X',Y',Z')-system the boomerang traverses an ordinary flight path, starting with the modified initial conditions. This trajectory can be transformed back to the old (X,Y,Z)-system according to:

$$\left.\begin{aligned} X(t) &= X'(t) + tW\cos\beta \\ Y(t) &= Y'(t) + tW\sin\beta \\ Z(t) &= Z'(t) \end{aligned}\right\} \quad (29.1)$$

where W is the constant wind speed. If W is very small, the modification of the initial conditions has little influence, and the main effect of the wind is that the velocity of the air is added to the velocity of the boomerang. If the flight lasts for a time T, the landing point is shifted downwind over a distance $\approx WT$. In reality the wind speed varies in space and time, but the above line of reasoning usually is qualitatively valid.

In fig. 29.3a through h flight paths are shown for boomerang 101.1 (level 2), which are computed with the initial conditions:
$f_o = 10$ rev/s, $V_o = 25$ m/s, $\Psi_o = 0°$,
$\vartheta_o = 80°$, $\varphi_o = 0°$, $\psi_o = -10°$,
$X_o = 0$ m, $Y_o = 0$ m, $Z_o = 1.8$ m,
β = variable, $W_o = 2$ m/s, $W_1 = 1$ m/s/10 m.
The values chosen for β are respectively: 0°, 45°, 90°, 135°, 180°, 225°, 270°, 315°.

β	V'_o	U'_o	Ψ'_o	D	Z_2
none	25.0	1.34	0.0	7.7	9.9
0°	27.1	1.45	0.0	27.1	13.0
45°	26.5	1.42	-3.3	20.0	12.6
90°	25.0	1.34	-4.9	14.6	10.6
135°	23.5	1.25	-3.7	17.9	8.2
180°	22.9	1.22	0.0	22.1	6.8
225°	23.6	1.26	3.7	25.0	7.4
270°	25.2	1.34	4.9	28.1	9.4
315°	26.6	1.42	3.3	28.8	11.7

table 29.2. Some values for the flights of fig. 29.3.

The wind speed at ground level $Z = 0$ is 2 m/s, at $Z = 10$ m: 3 m/s and at the launching point: 2.18 m/s. Values for the "modified initial conditions", V'_o, U'_o, Ψ'_o for these flights are listed in table 29.2 together with values for the maximum elevation Z_2 and the distance of the landing point D. In all 8 cases the average wind speed of about 2.5 m/s encountered by the boomerang spoils the return performance. Two main effects are visible: 1^{o} the boomerang is transported downwind, and 2^{o} the maximum height Z_2 increases with increasing values of cos $(\beta - \varphi)$, varying between 6.8 m for the throw downwind to 12.6 m for the throw upwind.

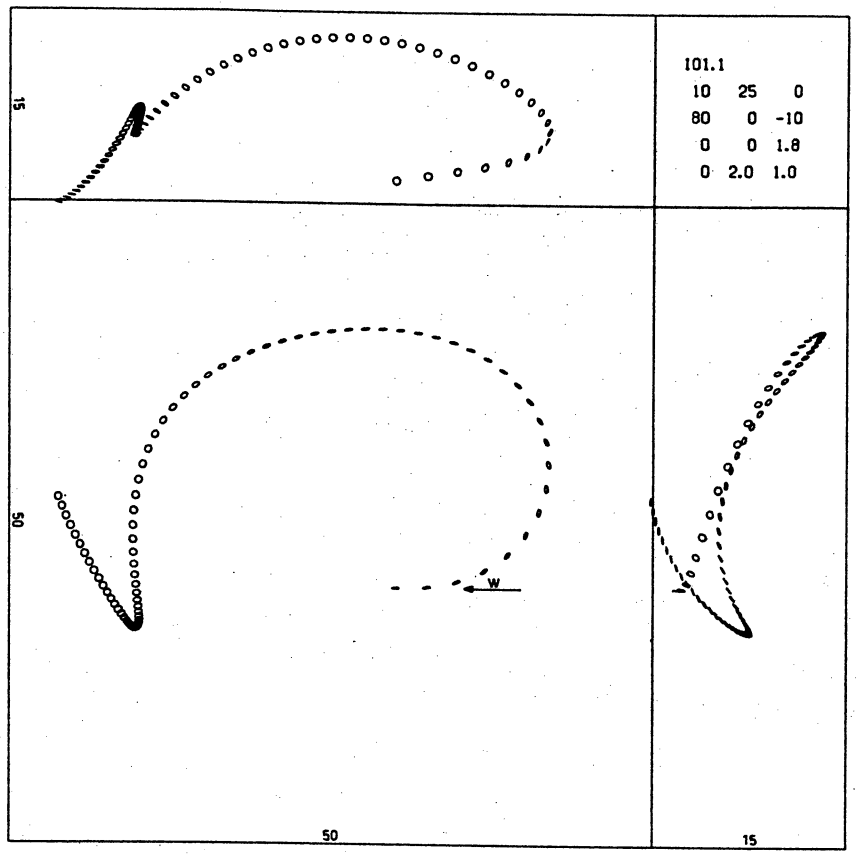

fig. 29.3a

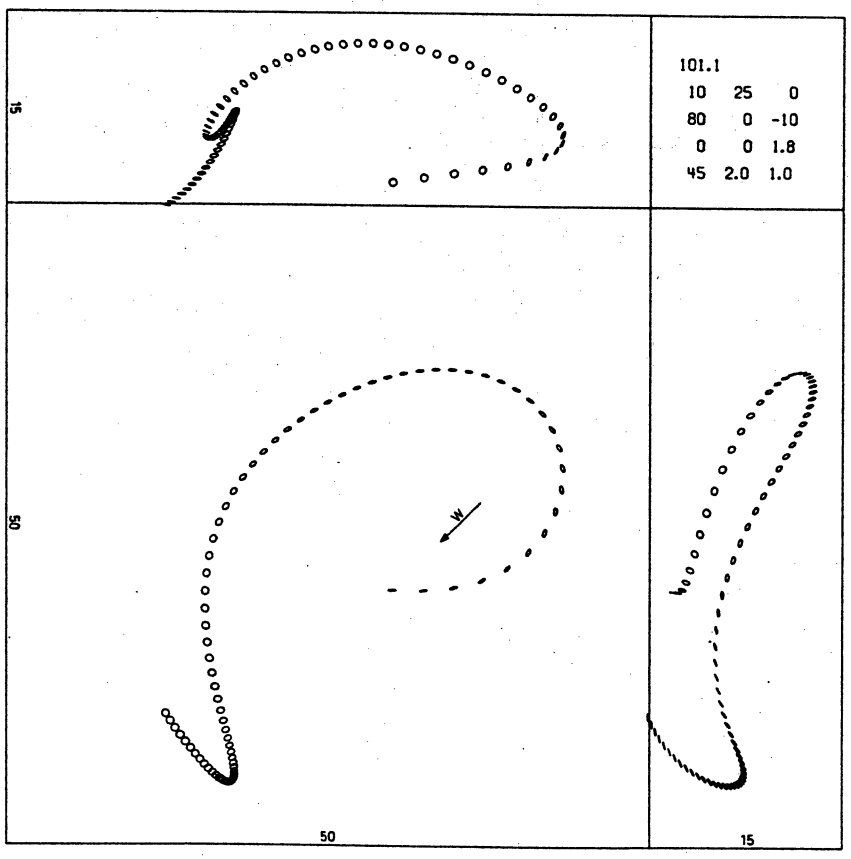

fig. 29.3b

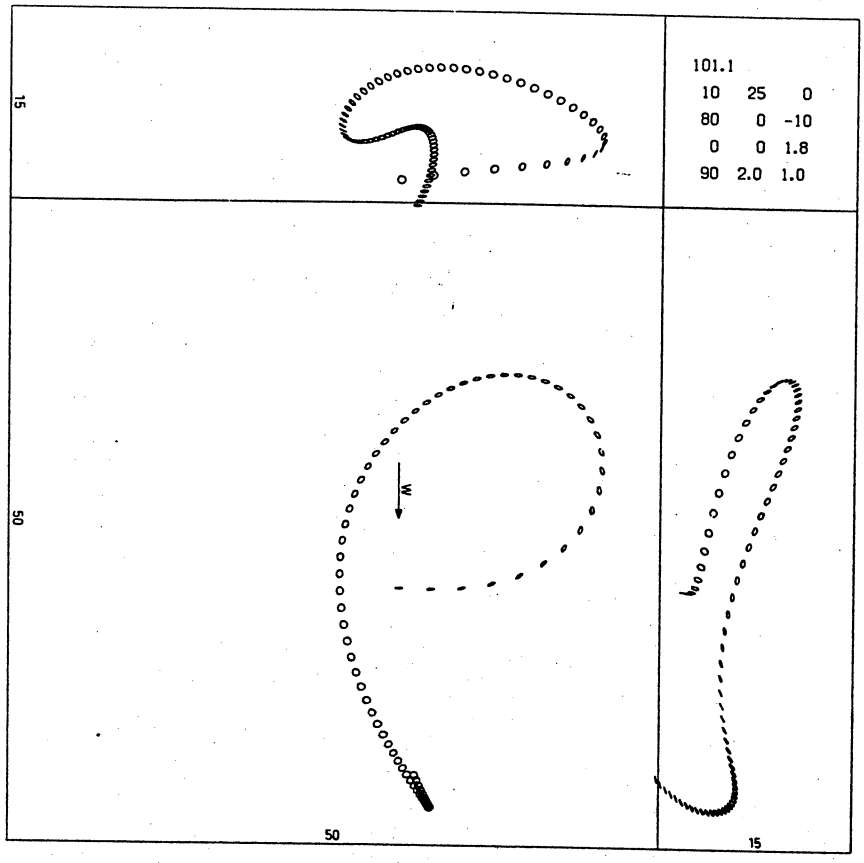

fig. 29.3c

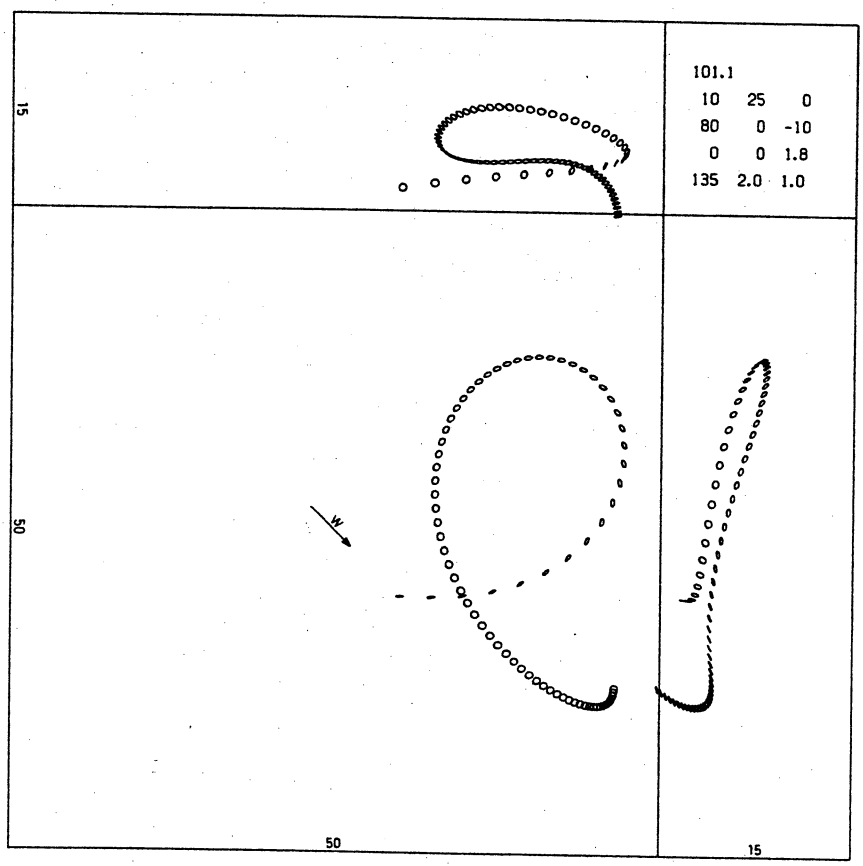

fig. 29.3d

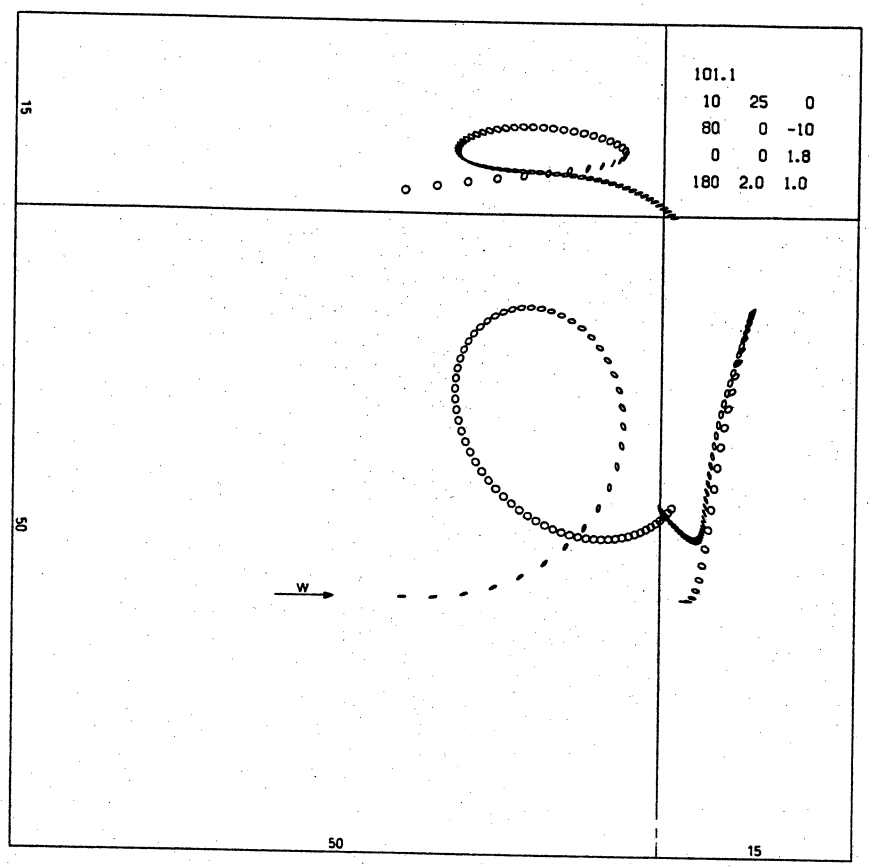

fig. 29.3e

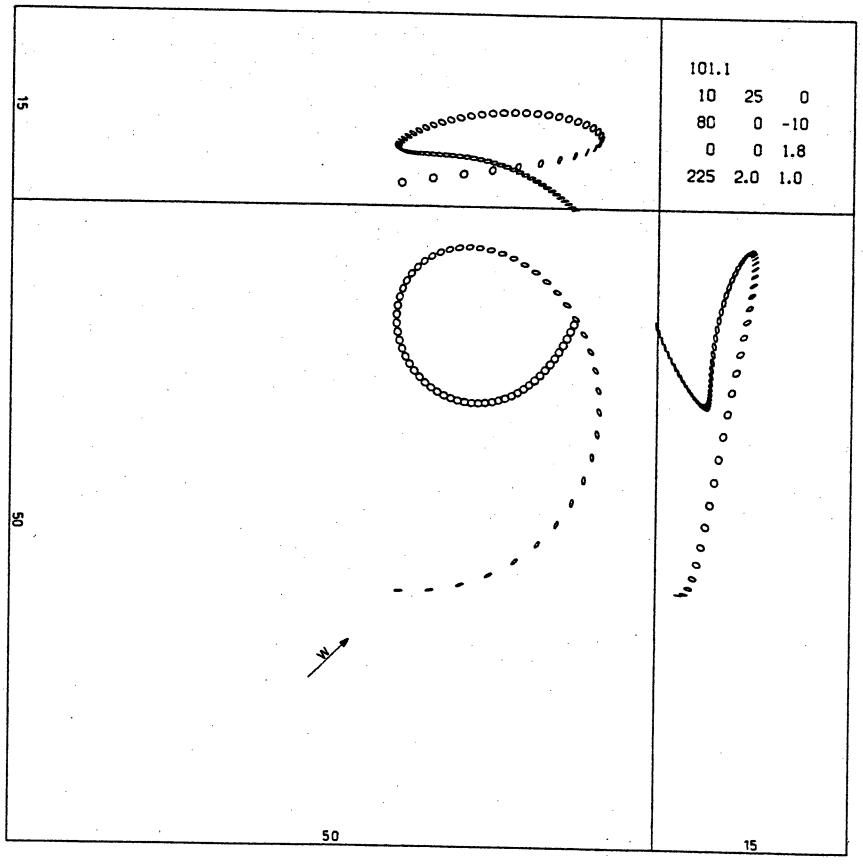

fig. 29.3f

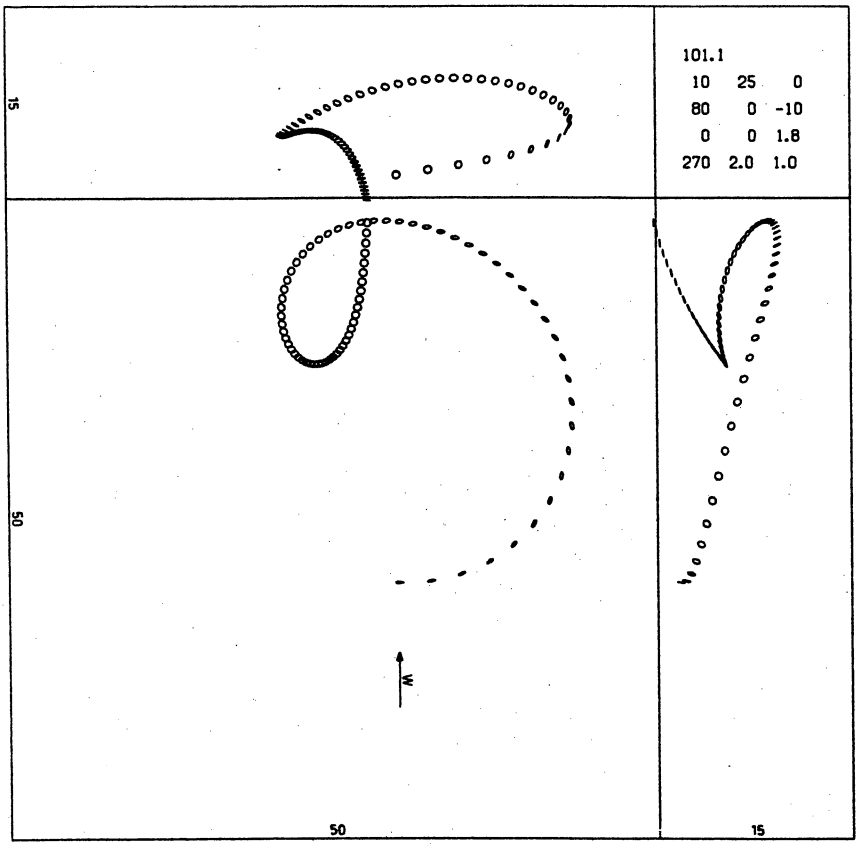

fig. 29.3g

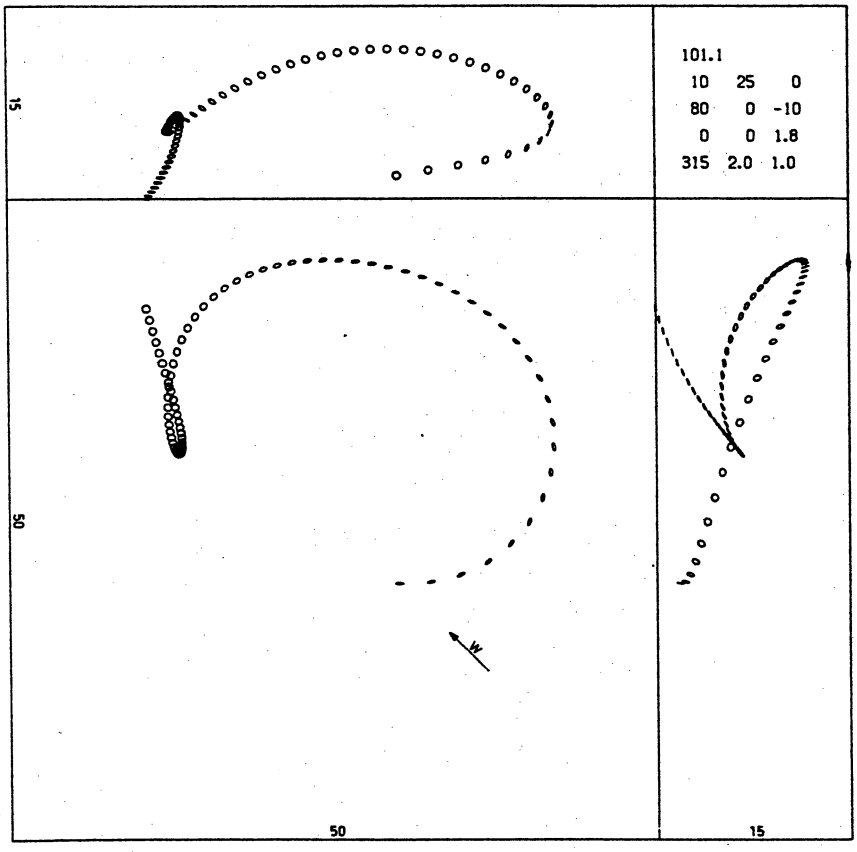

fig. 29.3h

§30 *Mass distribution: m and I_3.*

Two experimental examples showing the influence of a change in a boomerang's mass distribution on the diameter of the flight path are given in fig. 30.1 and fig. 30.2. These contain level 1 flight path stereograms for boomerang L1 plain and boomerang L1 weighted.

	a (m)	m (kg)	I_3 (kg. m^2)	λ
L1 plain	.298	.173	.00396	.258
L1 weighted	.298	.188	.00455	.272
difference	0	9%	15%	5.5%

Table 30.1. Mass distribution for L1 plain and L1 weighted. $\lambda = I_3/ma^2$.

The stereograms of fig. 30.1 are roughly similar in shape, they indicate a flight path diameter of about 22 m for the L1 plain, and about 28 m for the L1 weighted.

To investigate the influence of m and I_3 on boomerang flights, a number of model boomerangs were used, based on boomerang 101.1 (level 2), but with different values for m and I_3. They are listed in tabel 30.2. Boomerang 101.6 is almost identical with boomerang 101.1, the other six boomerangs differ by a factor 2 either in m or in I_3 or in both.

boomerang nr.	m (kg)	I_3 (kg. m^2)	λ
101.3	.080	.0020	.282
101.4	.160	.0020	.141
101.5	.080	.0040	.564
101.6	.160	.0040	.282
101.7	.320	.0040	.141
101.8	.160	.0080	.564
101.9	.320	.0080	.282

Table 30.2. Mass distributions for the 7 model boomerangs.

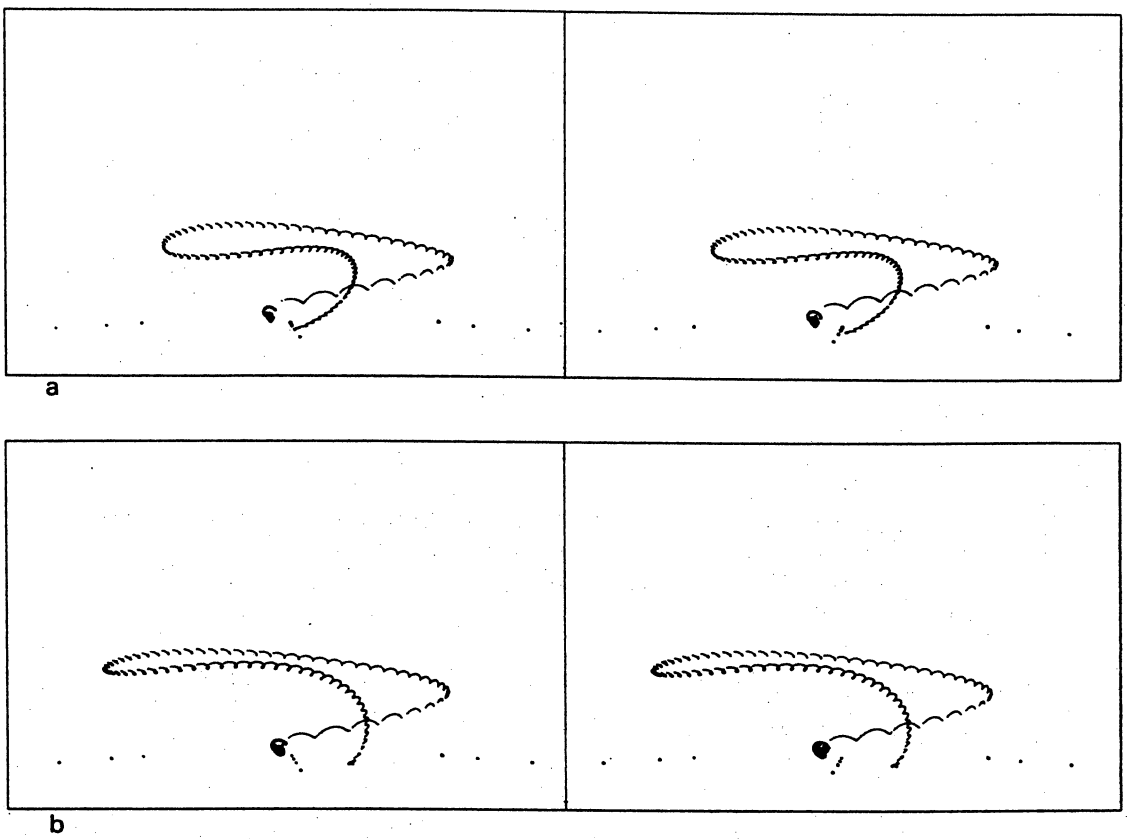

fig. 30.1. a: L1 plain, {1}, 7R6/L6A. b: L1 weighted, {1}, 11R19A/L19.

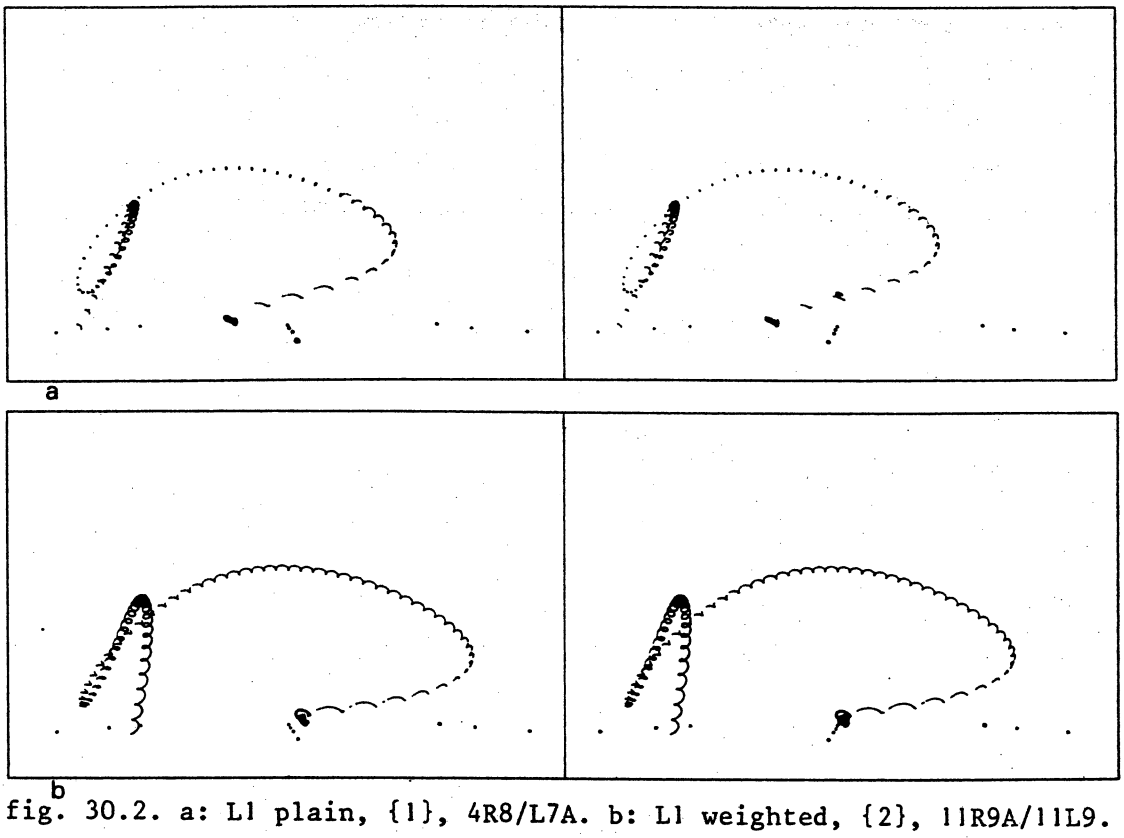

fig. 30.2. a: L1 plain, {1}, 4R8/L7A. b: L1 weighted, {2}, 11R9A/11L9.

Figure 30.1a through h shows 8 flight paths computed for these boomerangs. In 7 of these the initial conditions are:

$f_o = 10$ rev/s, $V_o = 25$ m/s, $\Psi_o = 0°$,

$\vartheta_o = 80°$, $\varphi_o = 0°$, $\psi_o = -10°$,

$X_o = 0$ m, $Y_o = 0$ m, $Z_o = 1.8$ m,

no wind.

The additional flight for boomerang 101.9 has the same initial conditions, except that $f_o = 12$ rev/s, $V_o = 30$ m/s.

bnr	t	P	n	D	Z_2	D_2	D_1	f_2	f_1	V_1	Ψ_2	U_1
101.3	8.4	66.9	56.4	3.6	9.6	11.6	1.3	10.0	5.9	2.1	24.2	.19
101.4	2.8	32.4	29.5	9.0	7.8	10.2	9.1	12.7	8.7	7.3	25.2	.34
101.5	7.7	85.1	49.8	21.9	3.5	33.5	19.0	10.0	5.5	4.0	20.2	.38
101.6	8.3	81.6	72.6	11.6	9.8	23.4	2.4	10.0	8.2	3.2	33.8	.20
101.7	3.2	41.1	37.6	17.6	7.1	21.5	17.6	12.7	9.9	7.4	28.1	.31
101.8	1.7	37.1	15.6	34.7	3.1	34.7	-	10.0	8.5	20.3	0.6	1.25
101.9	5.7	84.7	59.1	30.7	5.8	43.4	30.7	10.9	9.6	8.7	16.9	.43
101.9	9.2	125.9	106.9	12.0	11.5	45.6	10.4	12.2	11.3	4.2	45.0	.18

Table 30.3. Some values for the flights of fig. 30.1. Last row: $f_o = 12$, $V_o = 30$. Flight of 101.5 has minimum $\Psi = -1.2°$. Flight of 101.8 has minimum $\Psi = -0.7°$, D is increasing as the 101.8 reaches $Z = 0$.

Some values for the 8 flights of fig. 30.1 are listed in table 30.3. The relatively large differences in m and/or I_3 obviously give rise to dramatic differences in the shape of the flight paths. Boomerangs with equal values for λ have more or less similarly shaped flight paths which differ primarily in size. This rough similarity can also be observed in table 30.4, which lists some values of the flights at the instant at which $\dot{\Psi} = 0$ occurs for the first time. It is evident that boomerangs with low λ reach high values of Ψ and reversely. Again this phenomenon can be explained on the basis of the exposition given in the second half of §22.

In §7 it was shown that boomerangs such as 101.3, 101.6 and 101.9, which differ only in average density, but have the same λ, can traverse exactly similar flight paths, provided they are launched at the appropriate

bnr	t	f	V	U	Ψ
101.3	0.3	9.5	21.2	1.20	6.9
101.4	0.5	11.9	14.6	0.65	24.2
101.5	0.6	8.8	20.1	1.22	-1.2
101.6	0.8	9.5	19.4	1.09	7.8
101.7	1.0	11.9	13.6	0.61	28.1
101.8	0.5	9.5	22.6	1.27	-0.7
101.9	not reached				

Table 30.4. First instant t at which $\dot{\Psi} = 0$ occurs, and values of f,V,U,Ψ at that instant.

speed and spin. Suppose that, in accordance with table 7.1, row 3, we launch the three boomerangs with values for f_o and V_o as listed in table 30.5. Then we know that the flight path diameter for boomerang 101.3 is half that for boomerang 101.6, and that the flight path diameter of boomerang 101.9 is twice that for boomerang 101.6. The corresponding values for D_2 are listed in table 30.5. It is interesting to note that these values do not deviate much from those listed in table 30.3. This again shows that the flight path diameter is not very sensitive to the speed at which a boomerang is launched (provided that U_o is constant, see §26).

bnr	f_o	V_o	D_2
101.3	7.1	17.7	11.7
101.6	10.0	25.0	23.4
101.9	14.1	35.4	46.8

Table 30.5. Some values for similar flight paths.

It may be interesting to note the influence of the insertion of batteries in the elbow of an experimental boomerang. This increases m, but hardly I_3 (see §10). The addition of the batteries' mass causes the boomerang's angle of incidence to increase, which decreases the resulting flight path diameter. To a somewhat exaggerated degree this effect can be seen by comparing the computed flights for boomerangs 101.3 and 101.4 in fig. 30.3a and b, or the flights for boomerangs 101.5, 101.6 and 101.7 in fig. 30.3c,d and e.

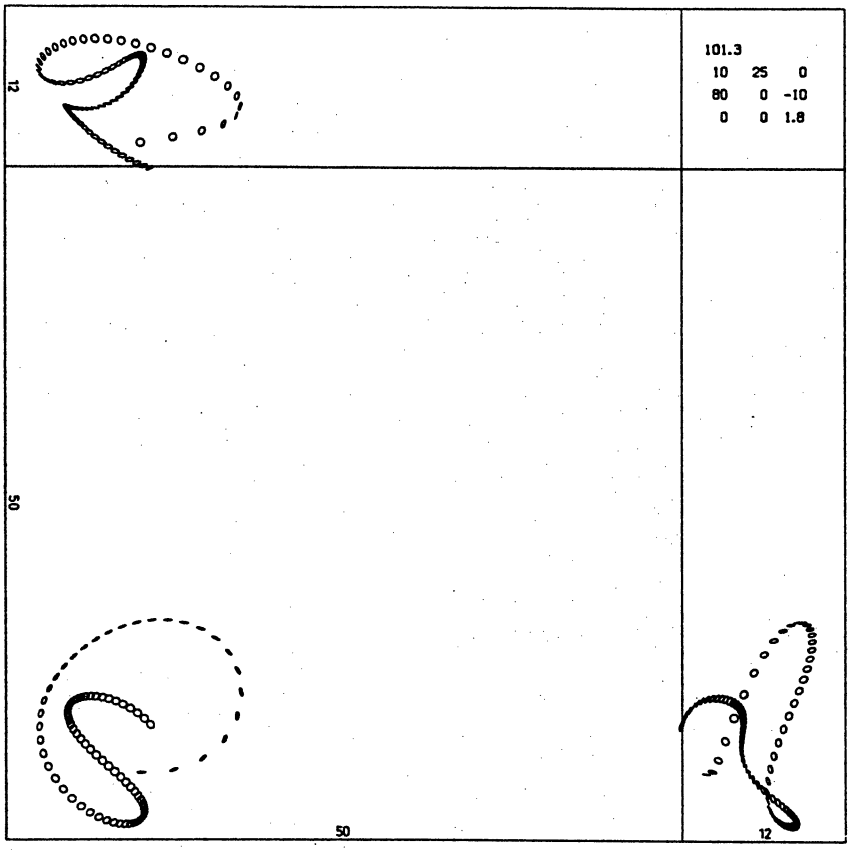

fig. 30.3a

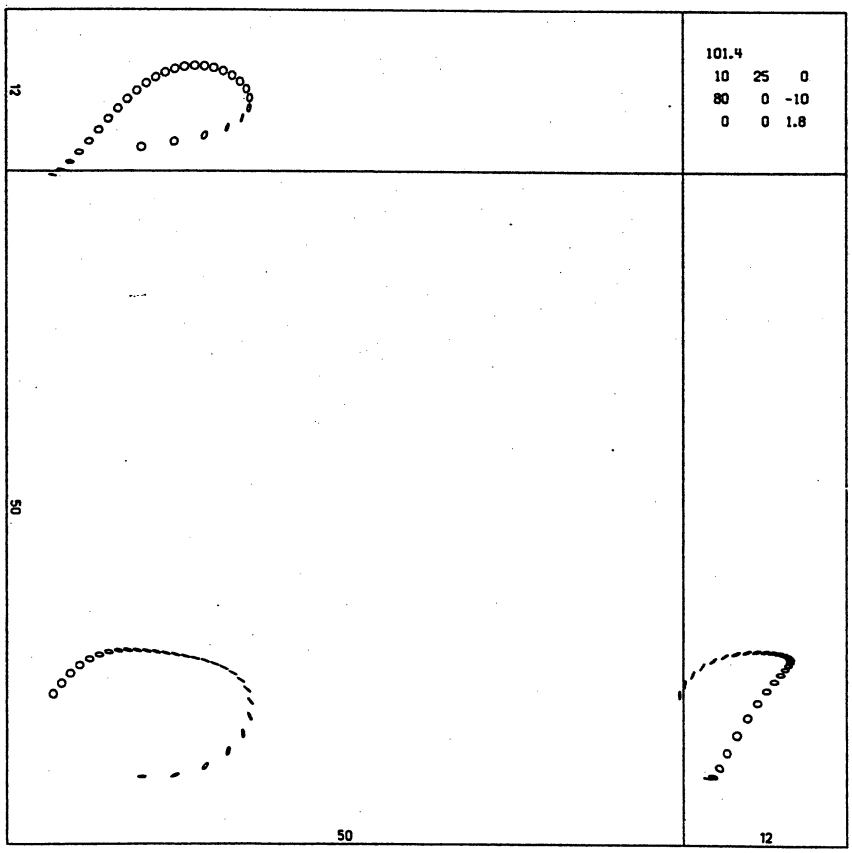

fig. 30.3b

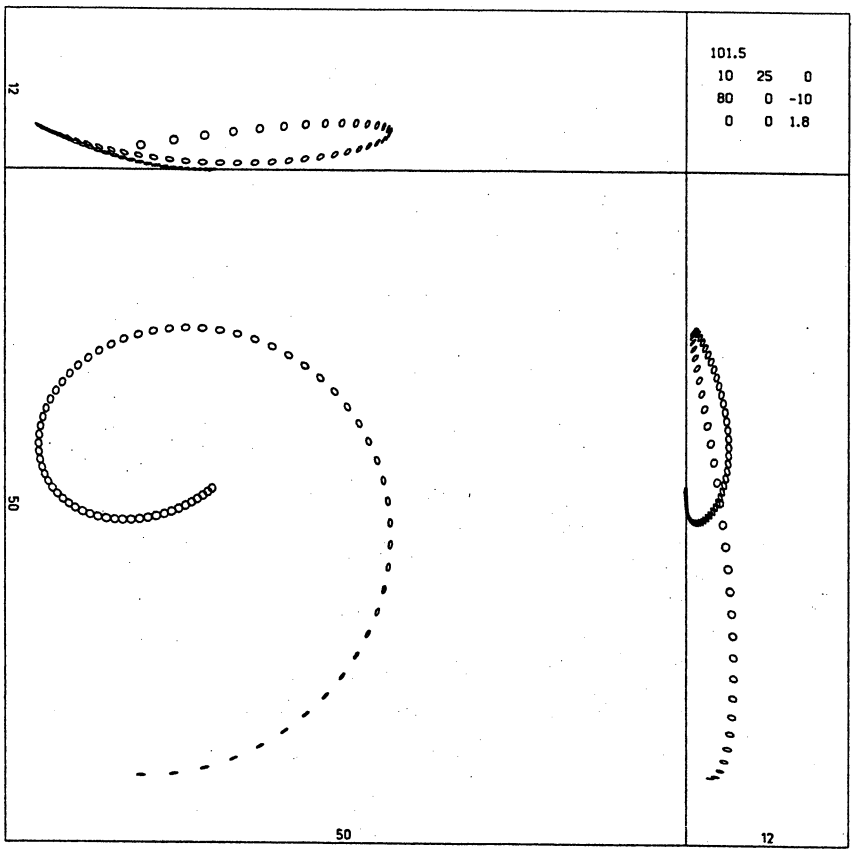

fig. 30.3c

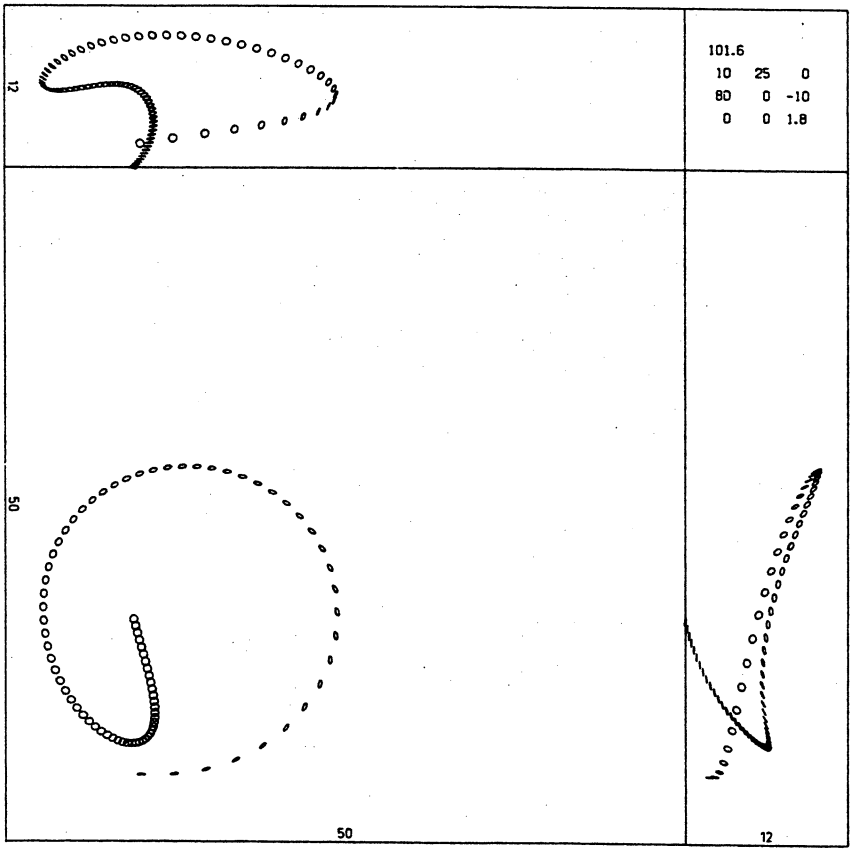

fig. 30.3d

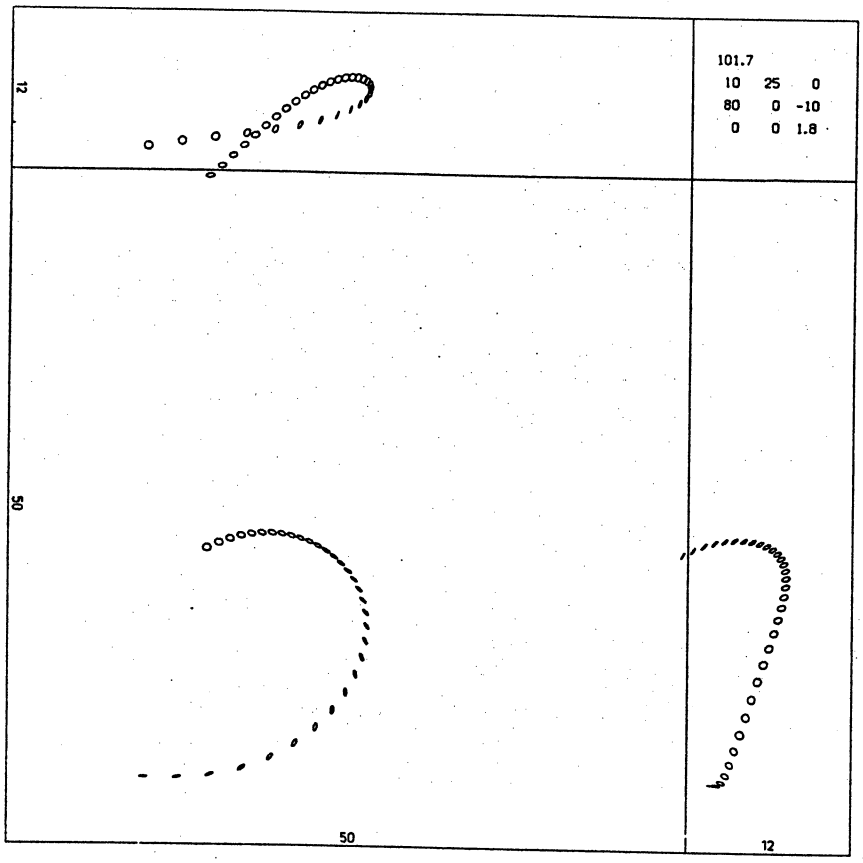

fig. 30.3e

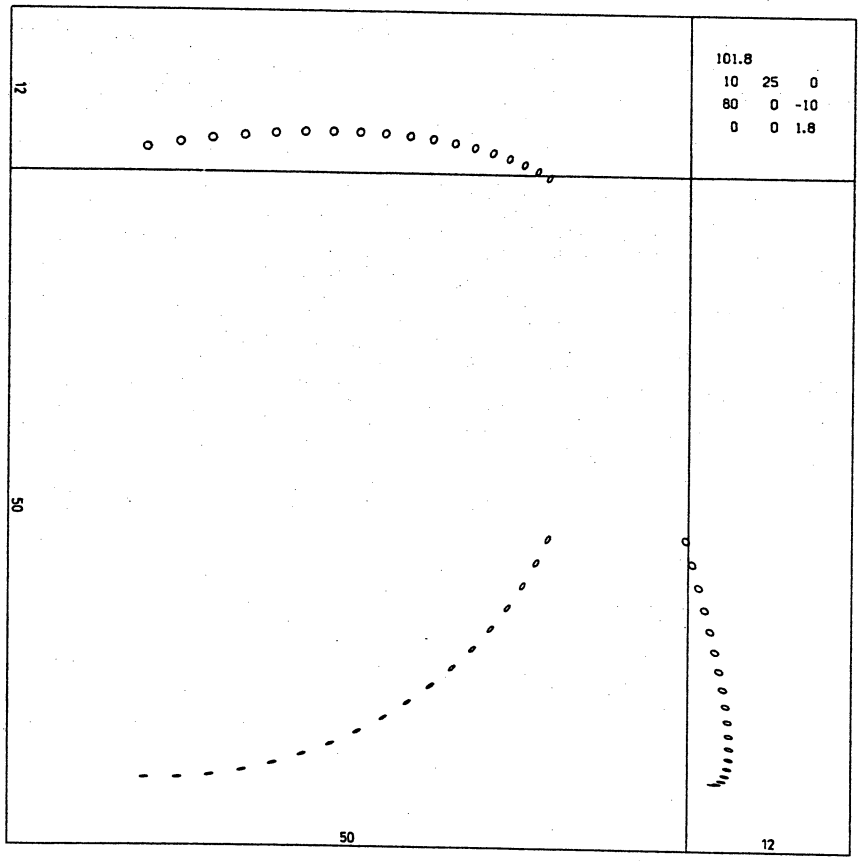

fig. 30.3f

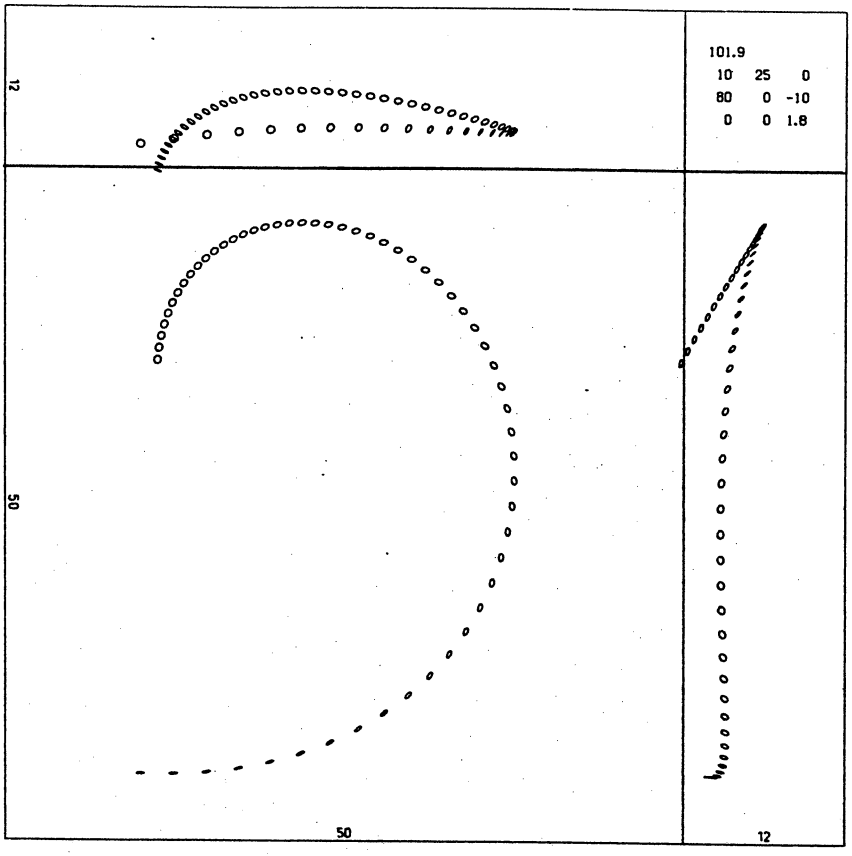

fig. 30.3g

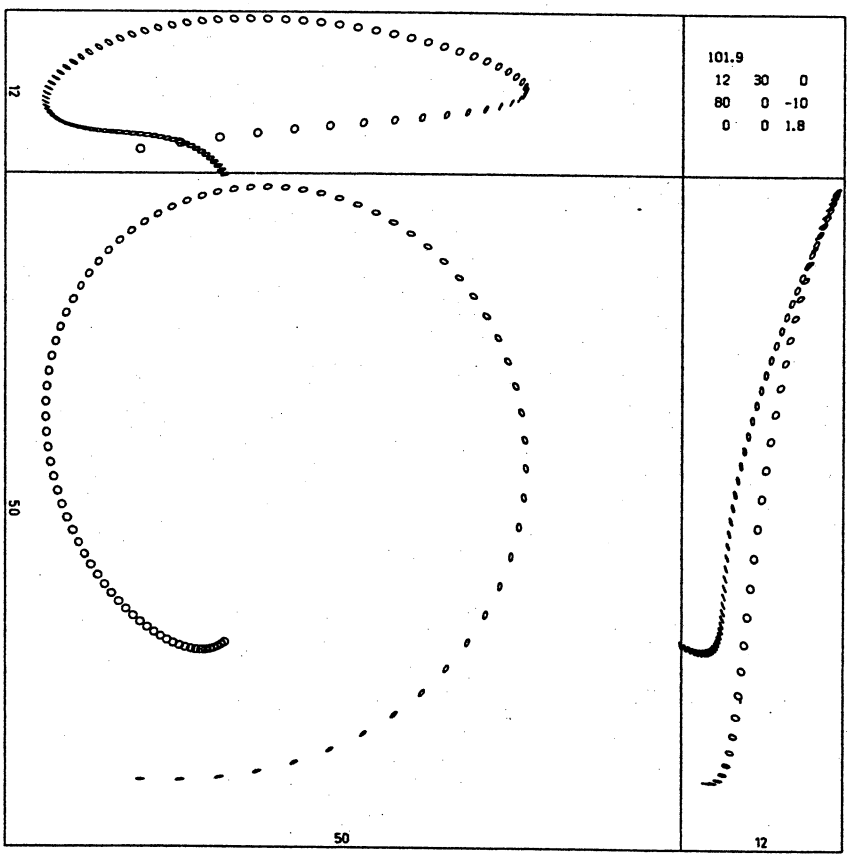

fig. 30.3h

§31 *Maximum lift coefficient* C_{L2}.

C_{L2} is the maximum lift coefficient for a boomerang arm's profile. In Part II, §22 the parameters characterizing the aerodynamic properties of level 3 model boomerangs are defined (see especially Part II, fig. 22.1). For moderate angles of incidence α^* ($\alpha_1 \leq \alpha^* \leq \alpha_2$) the profile lift coefficient C_L varies linearly with α^*. At $\alpha^* = \alpha_2$ C_L reaches its maximum value C_{L2}. For higher values of α^* stall occurs, and C_L decreases below C_{L2}.

The wind tunnel experiments reported in Part II, §26 indicated a value for C_{L2} of about 1.2 at most. The measurements were done on boomerang arms put in a straight airflow. In Part II, §32 it was shown that such low values of C_{L2} are unrealistic for boomerang arms forming part of *rotating* boomerangs. One of the reasons for including the present section is that it shows how poor the flight performance is of model boomerangs having arms with $C_{L2} = 1.2$.

boomerang nr.	normal profile C_{L2}	reversed profile C_{L2}
222.1	1.2	1.2
217.1	1.6	2.4
195.1	2.0	2.4
260.1	4.0	4.0

Table 31.1. C_{L2} values of model boomerangs.

Figure 31.1a through d shows 4 flight paths traversed by boomerangs differing only in C_{L2} and being otherwise identical with level 3 boomerang 195.1 (which is associated with boomerang L1 plain), see Part II, table 32.1. Table 31.1 lists the C_{L2} values for these boomerangs. The initial conditions in all 4 cases are:

$f_o = 11$ rev/s, $V_o = 27$ m/s, $\Psi_o = 0°$,
$\vartheta_o = 90°$, $\varphi_o = 0°$, $\Psi_o = -20°$,
$X_o = 0$ m, $Y_o = 0$ m, $Z_o = 1.8$ m,
no wind.